Toward Regenerating a Human Thumb In Situ

TISSUE ENGINEERING: Part A
Volume 15, Number 9, 2009

DOI: 10.1089/ten.tea.2008.0467

Original Article

Toward Regenerating a Human Thumb *In Situ*

Christian Weinand, M.D., Ph.D.,[1] Rajiv Gupta, Ph.D., M.D.,[2] Eli Weinberg, Ph.D.,[3] Ijad Madisch, M.D.,[2] Craig M. Neville, Ph.D.,[1] Jesse B. Jupiter, M.D.,[4] and Joseph P. Vacanti, M.D.[1]

Regenerative technology promises to alleviate the problem of limited donor supply for bone or organ transplants. Most expensive and time consuming is cell expansion in laboratories. We propose a method of magnetically enriched osteoprogenitor stem cells, dispersed in self-assembling hydrogels and applied onto new ultra-high-resolution, jet-based, three-dimensional printing of living human bone in a single-step for *in situ* bone regeneration. Human bone marrow–derived mesenchymal stem cells (hBMSCs) were enriched with CD 117^+ cells, dispersed in different collagen I and RAD 16I hydrogel mixes, and applied onto three-dimensional printed β-tricalcium phosphate/poly(lactic-co-glycolic acid) scaffolds, printed from ultra-high-resolution volumetric CT images of a human thumb. Constructs were directly implanted subcutaneously into nude mice for 6 weeks. *In vivo* radiographic volumetric CT scanning and histological evaluations were performed at 1, 2, 4, and 6 weeks, and expression of bone-specific genes and biomechanical compression testing at 6 weeks endpoint. Time-dependant accumulation of bone-like extracellular matrix was most evident in CD 117^+ hBMSCs using collagen I/RAD 16I hydrogel mix. This was shown histologically by Toluidine blue, von Kossa, and alkaline phosphatase staining, paralleled by increased radiological densities within implants approximating that of human bone, and confirmed by high expression of bone-specific osteonectin and biomechanical stiffness at 6 weeks. Human origin of newly formed tissue was established by expression of human *GAPDH* using RT-PCR. Statistical analysis confirmed high correlations between biomechanical stiffness, radiological densities, and bone markers. Bone tissue can be successfully regenerated *in vivo* using a single-step procedure with constructs composed of RAD 16I/collagen I hydrogel, CD 117^+–enriched hBMSCs, and porous β-tricalcium phosphate/poly(lactic-co-glycolic acid) scaffolds.

Introduction

Tissue regeneration is a promising approach to solve the problems of limited donor supply in organ and bone transplants. Especially, bone regeneration has shown promising progress when human bone marrow mesenchymal stromal cells are cultured with biodegradable scaffolds.[1] However, regeneration of complex, three-dimensional (3D) bones with the shape of human bones remains a big challenge due to the length of time required for proliferation of cells *in vitro*, to generate sufficient number of cells for tissue engineering bone *in vivo*.[2]

Human bone marrow–derived mesenchymal stem cells (hBMSCs) have a high proliferation potential and can be differentiated into osteoblasts.[1,3] Adult BMSCs are believed to divide asymmetrically producing a new multipotent stem cell and a unipotent progenitor cell that subsequently undergoes differentiation and maturation to form functional tissues such as bone.[4] In previous experiments, genetically altered monocultured immunoisolated CD 105^+ adult BMSCs have been demonstrated to regenerate bone successfully.[2] However, viral transfection of the cells was an additional costly laboratory step before use.[2] CD 117^+ hBMSCs represent a subpopulation of adult mesenchymal stem cells, are part of periosteal cells, and might have potential bone formation capacity.[5–8] The CD 117^+ epitope allows cell sorting and enrichment of hBMSCs with CD117^+ cells by magnetic antibody labeling. We hypothesized that low numbers of hBMSCs enriched with CD 117^+ cells have sufficient proliferation potential to allow for rapid expansion of enriched cell population to be used for *in situ* bone regeneration.

The microenvironment is likely to dictate the type of mature functional cells to regenerate new bone.[9–12] Hydrogels, a class of hydrated polymer and protein biomaterials, can be used to provide 3D microenvironment for cell growth.[13–19] Hydrogels can be tailored to regenerate specific tissues by

[1]Laboratory for Tissue Engineering and Organ Fabrication, Harvard Medical School, Massachusetts General Hospital, Boston, Massachusetts.
[2]Department of Radiology, Harvard Medical School, Massachusetts General Hospital, Charlestown, Massachusetts.
[3]Massachusetts Institute of Technology, Cambridge, Massachusetts.
[4]Hand and Upper Extremity Service, Harvard Medical School, Massachusetts General Hospital, Boston, Massachusetts.

incorporation of nutrients or biologically active molecules that direct functional differentiation and promote specific cell growth.[15,17,18] Given the strong metabolic demand of osteoblastic cells during mineralized tissue formation, effective nutrient delivery has long been considered an important factor for successful tissue engineering of bone.[16]

A new class of peptide-based biological hydrogels was discovered from studying self-assembling ionic self-complementary peptides, such as RAD 16I.[17] The peptides consist of alternating hydrophilic and hydrophobic amino acids, containing amino acid sequences that facilitate formation of hydrogel scaffolds with more than 99% water content (1–10 mg/mL). These alternating positive and negative charged regions allow for the stacking and nanofiber formation, resulting in β-sheet structures. RAD16I repeats the amino sequence Arginine-Alanine-Aspartate-Alanine four times.[19] The motif RAD was incorporated to mimic the known cell adhesion motif RGD that is found in many extracellular matrix (ECM) proteins. Work with these hydrogels has demonstrated that a variety of cells encapsulated and grown show functional differentiation and active migration, leading to extensive production of their own ECM.[18,19] These self-assembling peptides, including RAD 16I, assemble into nanofibers at physiological pH by altering NaCl or KCl concentration. Because resulting nanofibers are 1000-fold smaller than synthetic polymer microfibers, they surround cells in a manner similar to ECM. Hydrogels are an advantageous cell carrier as uniform cellular distribution is achieved when used on porous scaffolds, cell viability is sustained, and nutrients for tissue formation in scaffolds can be provided.[20–22] However, 1% RAD 16I hydrogel has a low viscosity preventing its application in regenerating shapes of bone. In our previous experiments, collagen I hydrogel has proven to be superior in supporting bone formation *in vitro* and *in vivo*.[23,24] We compared collagen I hydrogel as our standard in bone formation to RAD 16I and various mixtures of RAD 16I/collagen I to improve viscosity and probably shaped bone formation.

Hydrogels lack the initial mechanical strength needed to sustain the biomechanical stress for implantation *in vivo*, impeding their use alone as bone scaffolds. Many synthetic and natural materials, such as polyglycolic acid, β-tricalcium phosphate (β-TCP), poly (ε) caprolactone (PCL), and poly(lactic-co-glycolic acid) (PLGA),[25–29] provide the initial physical structure necessary for growth and differentiation of cells. However, they degrade eventually, allowing the cells to produce ECM components of their own. Ultimately, for defects with substantial curvature, the tissue-engineered constructs should also have matching topography.

Here materials that can be used for rapid 3D printing have the advantage of being printable in customized shapes to meet clinical demands. Rapid 3D printing uses a technology similar to ink-jet printing. From a computer-aided design (CAD) picture of the desired part, a slicing algorithm draws detailed information for every layer. Each layer begins with a thin distribution of powder spread over the surface of a powder bed. Using a technology similar to ink-jet printing, a binder material selectively joins particles where the object is to be formed. This layer-by-layer process repeats until the part is completed. After a heat treatment, unbound powder is removed, leaving the fabricated part. The support gained from the powder bed means that overhangs, undercuts, and internal volumes can be created (as long as there is a hole for the loose powder to escape). Material can be in a liquid carrier, or it can be applied as molten matter. The proper placement of droplets can be used to create surfaces of controlled texture and to control the internal microstructure of the printed part.[30] Consequently, we examined the combination of hydrogels as carriers to differentiate hBMSCs on the osteoinductive scaffold material TCP/PLGA.

To achieve new bone formation in highest detail of native bone, high-image resolution to engineer scaffolds is needed. The volumetric CT (VCT) is a new ultra-high isotropic spatial resolution ($150\times150\times150\,\mu m$) scanner that has not yet been evaluated in bone formation studies, but would prove to be an invaluable tool for this application. A parallel development of digital flat-panel detectors for conventional X-ray and mammography has provided ultra-high, spatial resolution, two-dimensional images. A VCT scanner combines the advances in CT with digital flat-panel detector technology. Unlike micro-CT, VCT is suitable for *in vivo* imaging of large animals and humans. High-resolution 3D imaging and quantitative capabilities of this new method can help detailed imaging of living bone to meet customer demands.

To prove the principle, we chose to tissue engineer the bones of a human thumb. The loss of the thumb in particular has a devastating effect on daily life.[31–35] In healthy children, focused effort should be made to replant the thumb.[31–35] However, digit injuries are often crushing or avulsing injuries of the bone and tissue, reducing chances of successful reattachment.[31–36] Thumb reconstruction techniques may be pursued, such as bone lengthening, bone grafting, toe-to-thumb transfer, or microvascular anastomosed joint transfer.[34–39] However, these options and outcomes are limited due to donor-site morbidity and in the availability of tissue.[34,35] Prosthetic joint reconstruction is available, but is not an attractive option, as it may be compromised by limited durability of the nonbiological materials or by intractable infection.[34,35] The ideal bone substitute would provide stability, motion, and durability without immunosuppressant.

To date, there have been few reports describing the engineered formation of bones with the shape of human bones such as the thumb.[40]

Materials and Methods

Human mesenchymal stem cells

Prior to the study, permission to use discarded tissue from operative surgeries was obtained from the Institutional Research Board Committee of the Massachusetts General Hospital. Bone marrow from human femoral heads was minced using a bone cutter, suspended in PBS, and filtered from debris through 100 μm and then 40 μm cell streamers. The marrow was then mixed into poligeline[41] and spun at 1 *g* for 40 min. The resultant supernatant was washed with PBS and used as follows.

hBMSC enrichment and CD 117$^+$ selection in vitro

Supernatant cells from human femoral heads were incubated with CD 117 antibodies attached to magnetic beads at 4°C for 15 min, according to manufacturer's instructions (Miltenyi Biotec, Auburn, CA), to allow antibodies to attach to epitopes. BMSCs were then enriched with labeled CD 117$^+$

cells by passing them through a magnetic field. CD 117^+–enriched BMSCs (hCD 117^+), CD 117^+–depleted cells (hCD 117^-), and untreated hBMSCs were labeled with FITC-labeled antibodies, and examined using fluorescent microscopy.

For selection of CD 117^+ cells, CD 117^+ antibody–labeled BMSCs in PBS were passed three times through the magnetic field. Thereby, a >95% purity was achieved.[41] Selected cells were tested for their ability to differentiate into cartilage, bone, and fat. About 2×10^5cells/mL were incubated with osteogenic medium (DMEM supplemented with 10% fetal bovine serum, 100 U/mL ampicillin, 100 μg/mL streptoreptomycin, 100 nM dexamethasone, 50 μg/mL ascorbic acid, and 10 mM β-glycerolphosphate [all from Sigma-Aldrich, St. Louis, MO, if not stated otherwise]) for 14 days, with chondrogenic medium (DMEM supplemented with 10% fetal bovine serum, 100 U/mL ampicillin, 100 μg/mL streptomycin, 10 ng/mL IGF-β1, 10^{-7}M dexamethasone, 50 μM ascorbate-2-phosphate, 40 μg/mL Proline, 100 μg/mL pyruvate, and 50 mg/mL ITS^+ Premix [Becton, Dickinson and Company, Franklin Lakes, NJ]) for 21 days, and with adipogenic medium (DMEM supplemented with 10% fetal bovine serum, 100 U/mL ampicillin, 100 μg/mL streptomycin, 0.5 mM isobutyl methylxanthine, 1 μM dexamethasone (Sigma-Aldrich), 10 μM insulin, 200 μM indomethacin, 100 U/mL ampicillin, and 100 μg/mL streptomycin) for 3 days. Bone was stained using Toluidine blue; cartilage, using Alcian blue; and fat, using Sudan red. Differentiated cells were evaluated by a histopathologist blinded to the study.

hCD 117^+ cells, hCD 117^- hBMSCs, and complete bone marrow cells were counted at outflow and mixed directly into a collagen I/RAD 16I mixes (75/25, 50/50, and 25/75) or collagen I at a concentration of 2×10^6cells/mL hydrogel. Previous experiments on different MSC cell concentrations in various hydrogels showed superior results for 2×10^6cells/mL for cell survival.[23,24] Therefore, we decided to use this cell concentration in our experiments.

In vitro *evaluation hydrogels*

We tested different mixtures of collagen I and RAD 16I hydrogels to increase viscosity, and evaluated the ability of the most suitable hydrogel mixture to support bone formation. Hydrogels were prepared as follows:

Collagen I hydrogel. (Cellagen™; ICN Biomedicals, Aurora, OH) was mixed on ice according to manufacturer's instructions using 5× concentrated osteogenic medium on ice. hBMSCs were mixed with liquid hydrogel, and 2 mL was placed onto each scaffold in a 37°C incubator. Gelation occurred after 1 min incubation.

RAD 16I hydrogel (3DMatrix, Cambridge, MA). One-percent hydrogel is a synthetic polypeptide that assembles into a 3D ECM after application of NaCl or KCl. The hydrogel was sonicated for 30 min in a bath sonicator (FS 30; Fisher Scientific, Pittsburgh, PA) to remove air bubbles and was diluted 1:1 (by volume) with cells suspended in 20% sucrose to adjust the pH. Collagen I hydrogel and RAD 16I were mixed 75:25, 50:50, and 25:75 to a final cell concentration of 2×10^6. Enriched cells were suspended in pure RAD 16I hydrogel and the RAD 16I/collagen I mixes at 37°C, and gelation time was measured.

After deciding on 25:75 RAD 16I/collagen I mixture as the most suitable combination for gelation, hCD 117^+ cells and hCD 117^- cells were dispersed into RAD 16I pure and RAD 16I/collagen I combination to evaluate cell proliferation and new bone formation. Hydrogel/cell mixes were incubated at 37°C in a CO_2 incubator. All cell–hydrogel mixes were examined under a light microscope every day, and samples were examined at 3 and 6 weeks for cell viability and bone formation, using H&E, alkaline phosphatase, von Kossa, and Toluidine blue staining, respectively, as well as the presence of osteoblasts and osteoclasts within the new formed tissue. No complete bone marrow was tested as CD 117^+ cells represent 2.5% of the entire bone marrow population.[42]

In vivo *experiment*

3D printed (3DP) human distal phalanx-shaped scaffolds—VCT imaging. An ultra-high-resolution VCT image was created from a right human cadaver hand, and proximal and distal phalanxes of the thumb were isolated. Digital reconstruction was performed by a slicing algorithm to draw detailed information for every layer into a 3D CAD picture (Fig. 1A,B). This image was transferred to a customized rapid 3D printer at Massachusetts Institute of Technology.

3DP β-TCP/PLGA distal and proximal phalanx scaffolds. The scaffolds comprised two parts (a distal phalanx and a proximal phalanx) and were printed three-dimensionally in a scale of 1:1. The materials used were a mixture of 50% PLGA (Boehringer-Ingelheim, Ridgefield, CT, LG824, PLGA 82:18 L:G, i.v. 1.7–2.6 dL/g) and 50% β-TCP (Cosmocel, San Nicolás de Los Garza, Mexico); the scaffold had an overall porosity of 90% with micropores of 100–250 μm (Fig. 1C–E). Both scaffolds had a net of channels of 1×1 mm throughout the entire scaffold to facilitate nutrient and cell delivery. The distal phalanx was 2.5 cm long in the exact shape of the ultra-high-resolution VCT image, and the proximal phalanx was 2.5 cm long. The proximal joint surface of the proximal phalanx scaffold was not printed due to a technical error in transmission from the VCT picture to the printer (Fig. 1C, D). All scaffolds were evaluated radiologically by VCT scan before implantation to attain baseline density.

Construct preparation and implantation

The Institutional Animal Care and Use Committee of the Massachusetts General Hospital approved all animal procedures.

Scaffolds were ETO sterilized with the scaffolds in a bag, allowing gas penetration. After sterilization, cold gas was allowed to evaporate, and the scaffolds were kept in sterile conditions under vacuum for 3 days until immediate use. hCD 117^+ cell/hydrogel suspensions were prepared as described above and applied onto the scaffold. Collagen I hydrogel with suspended hCD 117^+ cells served as standard to evaluate bone formation. Cellular controls comprised hCD 117^- suspended in RAD 16I/collagen I mix and collagen I hydrogel. Acellular controls were created with hydrogel only and scaffold material. Immediately upon gelation, constructs were implanted subcutaneously in the back of nude mice. From each group, four constructs were created, so a total of 28 mice were employed.

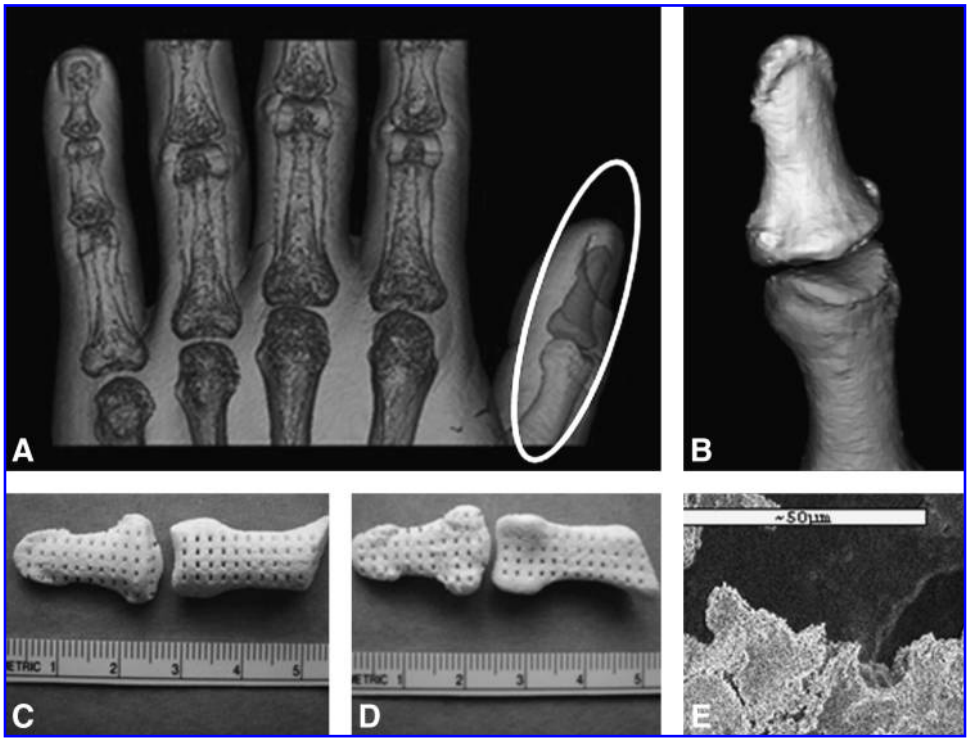

FIG. 1. (**A**) Three-dimensional volumetric CT (VCT) picture of the human hand; (**B**) volumetric reconstructed computer-aided design (CAD) image of human thumb; (**C, D**) macroscopical appearance, front and back, of the 3DP scaffold of the distal phalanx; (**E**) scanning electron microscopy picture of the scaffold. The bar represents 50 μm.

Six-to eight-week-old male nude mice (Charles-River Laboratories, Wilmington, MA) were anesthetized with Avertin 125–200 mg/kg IP. A dorsal subcutaneous pocket was formed, and one construct per mouse was implanted. The wound was closed with staples, each mouse received Buprenorphine 0.05–0.1 mg/kg intramuscularly, and animals were allowed to recover from surgery. Implanted constructs were processed over 6 weeks as described below.

Radiological evaluation

At 1, 2, 4, and 6 weeks, *in vivo* VCT scanning of each specimen was performed at 120 kV tube voltage and 10 mA tube current on a high-resolution VCT scanner (Siemens, Forchheim, Germany). The VCT scanner effective field of view was 25×25×18 cm, with isotropic resolution of ~200 m with 2×2 binning, and volumetric coverage. Projection data were reconstructed using a modified Feldkamp algorithm. To calculate mean values for bone formation of specimens, scaffolds were virtually separated into three parts of 0.8 cm length—tip, middle, and base. Radiological density of the samples was assessed measuring Hounsfield density units. Mean values were calculated using at least eight separate points from each sample. Mice were sacrificed at 6 weeks endpoint using an overdose of pentobarbital (200 mg/kg i.p.); constructs were explanted and processed.

Gross and histological evaluation

Next, specimens were harvested and examined for appearance. Specimens were cut into three parts of 0.8 cm length to assess bone formation through the length of the scaffold. From each part of each specimen, cuts of 0.1 cm thickness were taken from the proximal part of the scaffold and embedded into 10% phosphate-buffered formalin for histological analysis. Samples were decalcified and consequently embedded into paraffin; 4 μm sections were taken and evaluated histologically. Staining was done by H&E for cell morphology and viability, Toluidine blue for pericellular proteoglycan, alkaline phosphatase for bone tissue formation, and van Kossa staining on separate not decalcified samples of the new formed tissue. Histological evaluation of the samples was conducted by a histopathologist blinded to the study.

Biomechanical compression testing

Constructs were kept frozen separately until biomechanical testing. Each part was tested separately for compression using a Texture Analyzer TA-XT Plus (Texture Technologies, Scarsdale, NY), and corresponding parts were compared (referred to as tip, middle, and base). Unconstrained uniaxial compression was applied, while compressive force and displacement were recorded after the probe tip contacted the sample. Experiments were run until 35 kg limit of the load cell was reached. Geometry of the samples made measuring material moduli difficult, so we compared samples by referring to one sample that required higher force to compress as being stiffer than a sample that required less force to compress the same distance. Mean values for distal and proximal phalanxes of each construct were calculated combining values from tip, middle, and base.

Reverse transcriptase polymerase chain reaction (RT-PCR) analysis

For transcription analysis, total RNA was purified from samples with RNA STAT 60 according to the specifications of the manufacturer (Tel Test, Friendswood, TX). RNA was

quantified by spectrophotometric techniques, and integrity verified by observing ethidium bromide staining in a formaldehyde gel.[43] One μg of each sample was converted to cDNA in a 30 μL reaction containing 1× PCR buffer, 5 mM dNTPs, 0.5 μg random hexamer primers, and 200 U MMLV RT (Promega, Madison, WI). The reaction was subsequently heat-inactivated, and diluted to 100 μL with water. One-microliter aliquots were used in each 50 μL RT-PCR reaction, using gene-specific primers and 1 mM dUTP-biotin. After 22 cycles, 10 μL aliquots were fractionated on a 3% agarose gel (1% agarose and 2% NuSieve GTG agarose), blotted onto Amersham Hybond N^+ nitrocellulose filter, and probed with horseradish peroxidase–conjugated avidin (Sigma-Aldrich). The reaction was visualized using luminol substrate (Pierce Chemical, Rockford, IL) and autoradiography. Following primers were utilized:

Osteonectin (ON)—R, TTCCCCTCCTCCTGTTCTC; F, ACCCACCCGTCACTAAGACA
hGAPDH—R, GCCAGAGTTAAAAGCAGCC; F, GTTCGAGGACTGGTCCAAA
mGAPDH—R, GGAAGGCCATGCCAGTGAGC; F, CCTTCATTGACCTCAACTAC

Native human bone was used as control for transcription analysis. Films were digitized, and transcription levels for native swine bone were assigned a relative value of 1.

Statistical correlation analysis

Changes in the Hounsfield Units (HU) of each construct were correlated with biomechanical strength. Pearson, Kendall, and Spearman correlation coefficients were calculated, using MatLab 7.0 (The MathWorks, Natick, MA).

Results

In vitro *CD 117$^+$ cell evaluation*

CD 117^+ cells were FITC labeled to confirm enrichment of the cellular mixture (Fig. 2A), and a content of 1.5% to 2.7% was calculated for the femoral heads, dependant on their size. After enrichment, an increase of three- to fivefold of the CD 117^+ cells was observed, using MetaMorph (Expansion Programs International, Thunderstone, CA). Differentiation of the selected CD 117^+ cells to fat was observed after 3 days, using Sudan red staining, after 14 days to cartilage using Alcian blue stain for mucosubstances and acetic acids, and to bone using Toluidine blue stain for pericellular proteoglycan (Fig. 2B–D).

In vitro *hydrogel evaluation*

Collagen I hydrogel served as standard for viscosity for handling a hydrogel and gelation time. Gelation occurred within 2 min at 37°C. No deliberate change in shape was thereafter observed. Measured gelation times without deliberate change in shape of RAD 16I/collagen I hydrogel mixes 25:75, 50:50, and 75:25 were 2 min 35 s, 8 min 20 s, and nongelating at 37°C, respectively. The 25:75 RAD 16I/collacollagen I hydrogel mix was chosen for further evaluation and is referred to as RAD 16I/collagen I hydrogel in the following text. Cellular proliferation was supported by RAD 16I pure, collagen I, and RAD 16I/collagen I hydrogel at 3 and 6 weeks. Cells were viable in all hydrogels, confirmed by H&E staining. At 6 weeks endpoint new bone-like tissue formation in RAD 16I/collagen I hydrogels mixed with CD 117^+–enriched cells was confirmed by Toluidine blue, alkaline phosphatase, and von Kossa staining, and by the presence of osteocytes (Fig. 2E). Also, bone-like tissue was

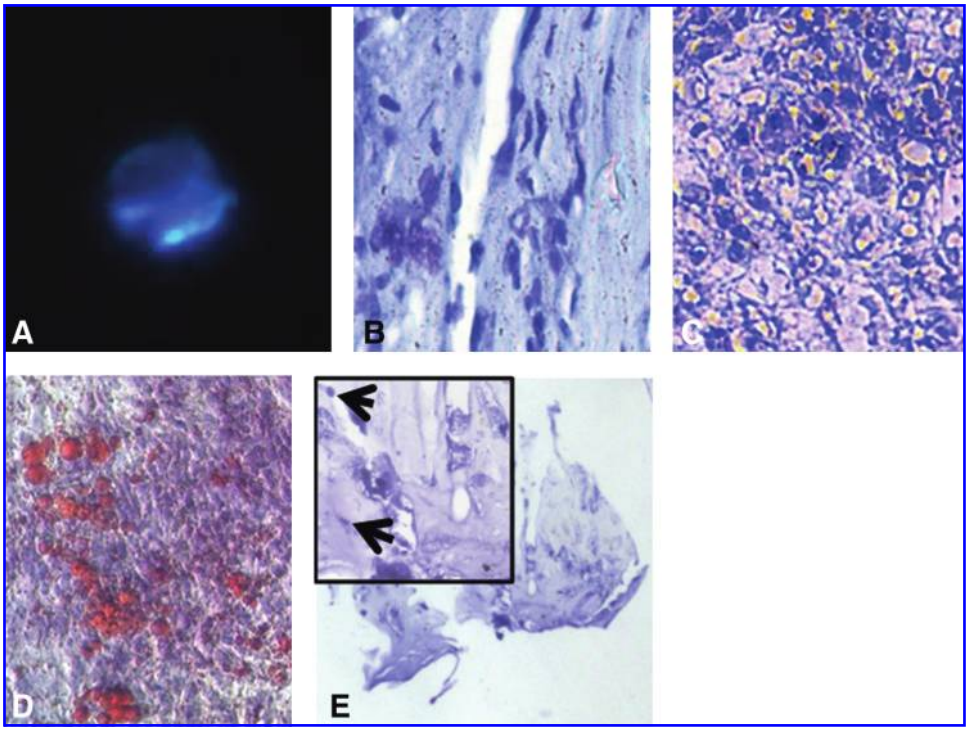

FIG. 2. (**A**) An FITC-labeled CD 117^+ cell, fluorescent microscope evaluation, 200× magnification; (**B–D**) osteogenic (Toluidine blue), chondrogenic (Alcian blue with eosin counterstain), and adipogenic (Sudan red) differentiation of CD 117^+ cells (magnification: 200×, 40×, and 40×, respectively); (**E**) CD 117^+ cells after 6 weeks in culture. Bone-like tissue with osteoblast—as well as osteoclast—like cells (arrows) is shown at 6 weeks endpoint by positively staining for pericellular proteoglycans, using Toluidine blue stain (magnification: 40× and 100×). Color images available online at www.liebertonline.com/ten.

formed by hCD 117$^-$ cells and complete bone marrow cells; however, staining was lesser than using CD 117$^+$–enriched cells (results not shown).

In vivo: *β-TCP/PLGA scaffold–distal and proximal phalanges*

All mice survived until the predetermined endpoint of 6 weeks. No infections were noted.

CD 117$^+$–enriched cells in collagen/RAD 16I hydrogel and collagen I hydrogel

VCT scanning. At implantation, similar densities of cellular and acellular scaffolds were recorded. During 6 weeks *in vivo* scanning, cellular specimens showed significantly higher densities than acellular control groups. The highest increase in density was observed in samples composed of hCD 117$^+$ in collagen I/RAD 16I hydrogel. Constructs had an average density of 341.2 HU (minimum, 204.0 HU; maximum, 1170.0 HU). The scaffold with CD 117$^+$–enriched cells/collagen I had a mean density of 247.5 HU (minimum, 193.0 HU; maximum, 361.8 HU) (Figs. 3A and 5A). Maximum density in these constructs was comparable to that of native human bone in the hand (Fig. 3A, B).

Histological evaluation. After explantation, scaffold material was still present; shape and length had not changed (2.5 cm each). Channels were filled with new formed tissue. Distal and proximal phalanx scaffolds were clearly separated from each other. However, thin layers of fibrous tissue partially connected them at the joint. Interestingly, this fibrous layer was only noted on hCD 117$^+$ specimens. During coronal cutting in three pieces of 0.8 cm length, specimens with hCD 117$^+$ in collagen I/RAD 16I and collagen I had the highest resistance.

Specimens were entirely surrounded and penetrated with new cortical bone-like tissue. Cells in the surrounding tissue had elongated spindle-shaped osteocyte-like morphology with basophilic cytoplasm. Cut specimens showed newly formed tissue with areas of lamellar bone formation and cells in the new tissue that had more round basophilic osteoblast-like morphology. The tip of the distal phalanx was completely penetrated with newly formed bone-like tissue, resembling cortical bone. Collagen I specimens were also surrounded by newly formed tissue, but to a lesser degree than the collagen I/RAD 16I specimens. This tissue stained positive with Toluidine blue, alkaline phosphatase, and von Kossa (Fig. 4A).

Unconstrained uniaxial compression testing. Unconstrained uniaxial compression testing was concordant to radiological and histological findings. The highest stiffness was in the collagen I/RAD 16I samples in the distal phalanx tip, and lesser stiffness was measured in the proximal phalanx. Collagen I specimens had lesser stiffness. Highest stiffness in both hydrogel groups was noted for the tip of the distal phalanges, concordant with radiological densities (Fig. 5B).

RT-PCR. Expression of ON was highest in collagen I/RAD 16I hydrogels. Specimens of enriched cells in collagen I hydrogel showed lesser expression of the ON (Fig. 6A, B, and Table. 1). Human *GAPDH* expression was up to 85% in implanted constructs, and mouse *GAPDH* less than 1%, confirming human origin of the new tissue (Table 1).

hCD 117$^-$ in collagen/RAD 16I hydrogel and collagen I hydrogel

VCT scanning. Constructs showed lesser densities than corresponding hydrogel samples with CD 117$^+$–enriched cell populations, although this difference did not reach statistical significance. In VCT images, densities of cellular scaffolds were visually as well as quantitatively higher than acellular scaffolds (Fig. 5A). Samples made with collagen I/RAD 16I hydrogel showed at 6 weeks higher HU densities than samples in collagen I hydrogel. No difference was noted between the distal and proximal phalanxes of each construct.

Histological evaluation. Tissue surrounding explanted specimens was confirmed to be new bone-like tissue by Toluidine blue, alkaline phosphatase, and von Kossa staining. Both scaffolds had maintained length and diameter after 6 weeks. Channels were filled with new formed tissue but less dense than CD 117$^+$–enriched samples. This tissue inside the channels also stained positive for bone by van Kossa, alkaline phosphatase, and Toluidine blue staining. Cells in the tissue filling the channels had a round basophilic osteocyte-like appearance. In addition, fibrous tissue was noted within the bone-like tissue, and cells were eosinophilic, elongated with a spindle-like shape and staining negative for bone (Fig. 4C, D). Histologically, no difference between the

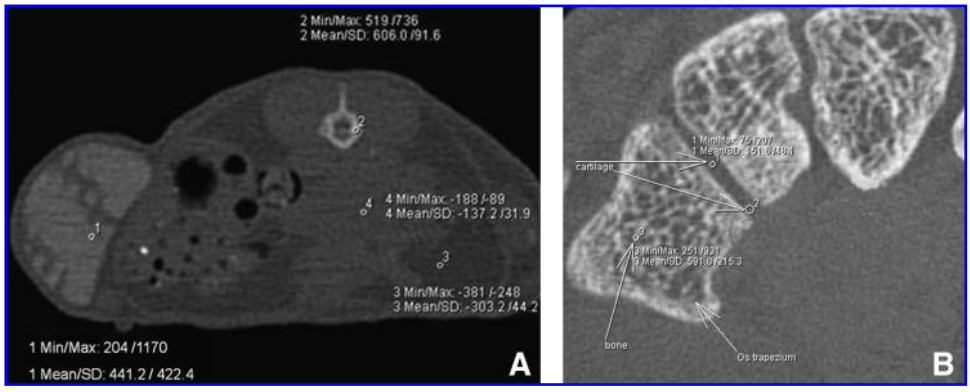

FIG. 3. (**A**) *In vivo* coronal cut via VCT through the mouse with the implanted construct *in vivo* supplying Hounsfield densities within the newly formed tissue after 6 weeks. The newly formed tissue shows Hounsfield densities within the range of native bone. (**B**) Coronal cut from a VCT image of a human hand *in vivo*, enabling a comparison of the Hounsfield densities of human bone in a human hand *in vivo* to the construct in (**A**).

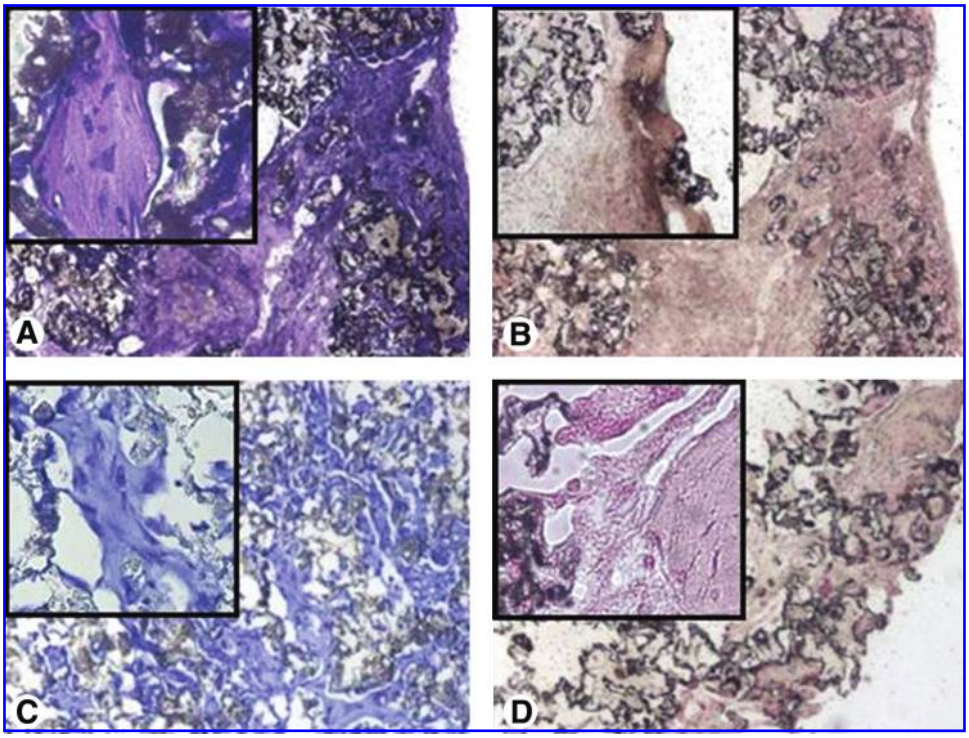

FIG. 4. Histological evaluation after explantation of the TCP/PLGA with collagen I/RAD 16I hydrogel mix with CD 117^+–enriched hMSCs compared to CD 117–depleted hMSCs after 6 weeks *in vivo*. The newly formed bone-like tissue integrates into the scaffold material (magnification: 40× and 200× (**A**), 40× and 100× (**B**)). Toluidine blue (**A, C**) and von Kossa (**B, D**) staining; CD 117^+–depleted collagen I/RAD 16I mix after 6 weeks *in vivo*. Newly formed fibrous and bone-like tissue integrating into the scaffold material (magnification: 40× and 200× (C), 40× and 100× (D)). Toluidine blue (**C**) and von Kossa (**D**) staining. Color images available online at www.liebertonline.com/ten.

samples of the two different hydrogels was noted in tissue formation.

Unconstrained uniaxial compression testing. Specimens of the two hydrogel groups showed similar biomechanical stiffness. Collagen I specimens showed greater variability in stiffness than collagen I/RAD 16I specimens (Fig. 5B). The distal tip of the phalanx of both specimen hydrogel groups had higher stiffness than middle and base. Specimens had statistically significant ($p < 0.05$) lesser stiffness than

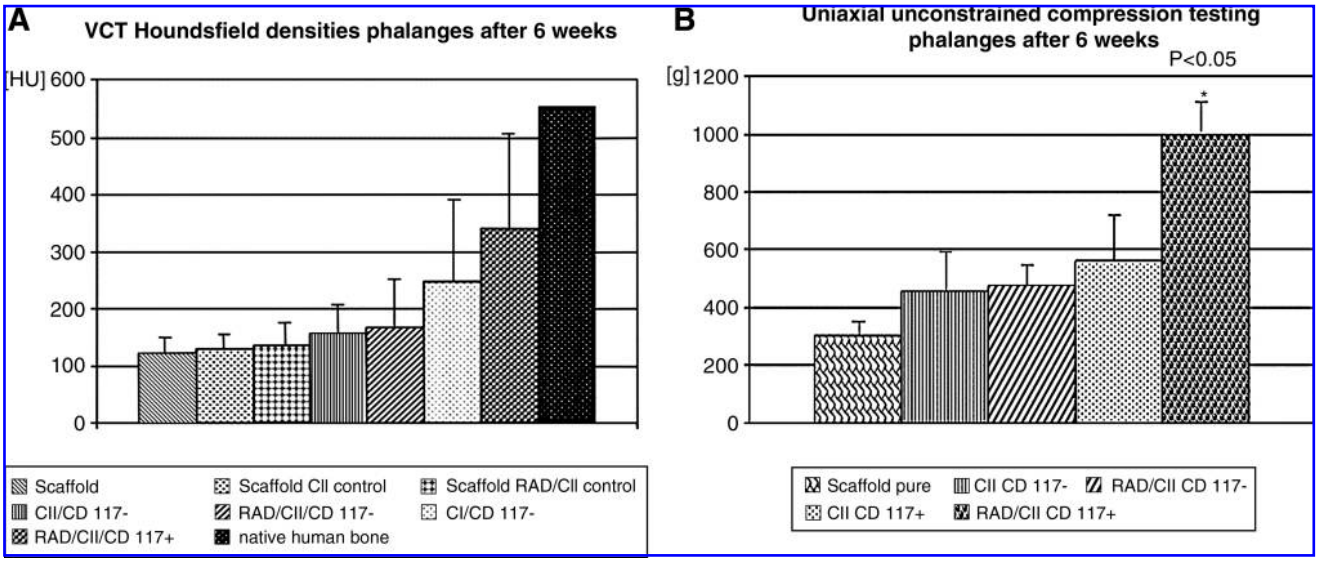

FIG. 5. (**A**) Hounsfield units at 6 weeks *in vivo*, measured in constructs with CD 117^+–enriched cells (CD 117^+) in RAD 16I/collagen I mix (RAD/CII) or collagen I hydrogel (CII) and controls. CD 117^+–enriched cells in RAD 16I/collagen I have the highest values, while the scaffold has the lowest density values. CD 117^-, CD 117^+–depleted cells; Scaffold RAD/CII control, acellular control with RAD 16I/collagen I hydrogel; Scaffold CII, acellular control with collagen I hydrogel. (**B**) Biomechanical compression testing of the constructs. The specimen composed of CD 117^+–enriched cells in RAD 16I/collagen I (RAD/CII/CD117^+) has the highest stiffness. CII/CD 117^+, collagen I with CD 117^+–enriched cells; cII+cells, collagen I cellular specimen; cII+PM+cells, collagen I/RAD 16I cellular specimen; control, collagen I/RAD 16I control; scaffold pure, scaffold without hydrogel and cells.

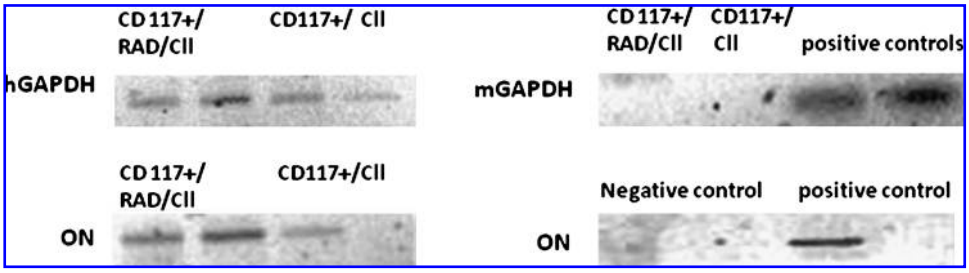

FIG. 6. Expression of the householding gene *GAPDH* in controls and in the constructs for human cells (hGAPDH) or mouse cells (mGAPDH). The constructs only showed expression of hGAPDH; expression of osteonectin (ON) as marker for mature bone in the constructs and controls. CD 117^+–enriched cell samples in RAD 16I/collagen I mix expressed the highest values. CD 117^+/CII, CD 117^+–enriched cells in collagen I.

constructs from CD 117^+–enriched cells with collagen I/RAD 16I; however, no statistically significant difference was noted to collagen I samples with CD 117^+–enriched cells.

RT-PCR. In these specimens also, human *GAPDH* expression was more than 85% and mouse *GAPDH* 1%, confirming origin of the new tissue to be human. ON expression of more than 50% was similar in specimens of both hydrogels tested (results not shown).

Acellular controls

VCT scanning. A mean density of 157.0 HU was measured in collagen I/RAD 16I acellular constructs; acellular collagen I specimens showed similar densities of 136.1 HU at 6 weeks, significantly lesser than cellular constructs made from CD 117^+–enriched cells with collagen I/RAD 16I hydrogels (Fig. 5A).

Histological evaluation. At explantation, controls also had maintained their shape and size. Some new tissue was noted surrounding the samples, no difference of the tissue was noted between the two hydrogels. Acellular hydrogel controls showed invasion of small, round eosinophilic lymphocyte-like cells and were surrounded by newly formed fibrous tissue with elongated spindle-shaped fibrocyte-like cells. Plain scaffold without hydrogel and cells showed fibrous tissue within the material and surrounding the scaffold, composed of elongated eosinophilic fibroblast-like cells and small, round eosinophilic lymphocyte-like cells. However, these tissues stained negative for bone with Toluidine blue, alkaline phosphatase, and von Kossa.

Table 1. Quantitative Analysis

	RAD/Coll CD 117+	*Coll1 CD 117+*	*Human Bone*
Osteonectin (ON)	0.89 ± 0.1	0.42 ± 0.15	1
hGAPDH	0.74 ± 0.12	0.70 ± 0.12	1
mGAPDH	0.01 ± 0.01	0.01 ± 0.01	0

Tissue-engineered bone in RAD 16I/collagen I hydrogel has values closest to native bone. The values represent from top to bottom: osteonectin, human GAPDH (hGAPDH), and mouse GADPH (mGAPDH).

Unconstrained uniaxial compression testing. Cellular specimens had higher stiffness than acellular controls. These findings were concordant with histological and radiological results. Controls without hydrogel and cells had the lowest stiffness (Fig. 5B).

Statistical correlation analysis

Higher HU corresponded to increased biomechanical strength of both distal and proximal phalanges (Spearman correlation 0.800, Pearson 0.72, and Kendall 0.667). This association was robust across the different correlation coefficients.

Discussion

Successful tissue engineering involves the implantation of living cells within synthetic scaffolds for the generation of new tissue. We have tissue engineered phalanges of a human thumb, using a novel 3DP technique. This revolutionary technique of rapid processing allows construction of forms in any desired shape as long as there is a CT image available. Quality of the scaffold depends on the resolution of the CT scanner. Our phalanges were constructed based on images using an ultra-high-resolution scanner, which is an excellent tool for this purpose. We chose the distal phalanx for the first engineering attempt since our laboratory had experience with similar approaches.[40] In contrast to previous work, we were able to print an exact anatomical scaffold using the ultra-high-resolution technique of the new VCT scanner to create a detailed picture. Details of each scaffold were confirmed by VCT scanning before application of the hydrogel/cell mix.

Ideal scaffold materials in tissue engineering should have a degradation rate matching the rate of tissue regeneration. Synthetic materials such as PCL often used in tissue engineering are only known to be osteoconductive and have a degradation rate of 2 years.[26,29] Therefore, newly formed bone-like tissue cannot easily replace the scaffold material. Calcium-derived biomaterials are osteoinductive[44] and can be combined with PLGA,[45] degrading at a faster rate than PCL.[26,29,45] We found that β-TCP/PLGA scaffolds combine osteoinductivity and osteoconductivity. PLGA adds flexibility to brittle β-TCP, thereby improving utility of scaffolds. We did not observe changes in shape or size in the scaffold material, possibly due to the degradation rate of PLGA within 2 months, comparable to β-TCP.[44,45] Our biodegradable

scaffold was 3DP from β-TCP and PLGA, which are proven to be osteoinductive and osteoconductive, and to provide some strength to the repair site *in vivo*.[45–47] This material mix has not been tested so far, but our results show that combining scaffold with our hydrogel mix and hCD 117$^+$ cell population forms histological bone-like tissue.

CD 117$^+$ cells have been described in literature as part of the periosteum, and the epitope is expressed in mesenchymal stem cells.[5–8] As periosteal cells, CD 117$^+$ cells are very likely to participate in bone formation, especially as they are mesenchymal stem cells and they have bone formation potential, as we have shown in our experiment. However, these cells represent a subpopulation of 2.5% of BMSCs.[42] This number was concordant to our findings. Due to the small number of CD 117$^+$ cells in bone marrow, we decided not to test complete human bone marrow as control. Human bone marrow itself harvested from femoral site provides 20 colony forming units of hMSCs.[48] In a previous experiment we have shown that small numbers of BMSCs as used in the current experiment are not capable to support bone regeneration *in situ* (results not shown); therefore, a different approach is needed. Possible solutions are increasing numbers of mesenchymal progenitor cells involved in bone formation,[49] or transfecting BMSCs for delivery of protein.[2] However, transfection and culture expansion are costly and time consuming, and loss of multipotentiality with spontaneous transformation of cultured stem cells *ex vivo* is described.[50] Based on our previous experiments with MSCs in various hydrogels on bone formation[23,24] and as CD 117$^+$ cells are involved in bone formation,[5–8] we decided on testing a magnetically enriched number of CD 117$^+$ cells in hydrogels for the best bone regeneration *in situ*. Using this approach, time-consuming step of cellular expansion in the laboratory could be eliminated.

Our engineering approach might be comparable to healing of fractured bone. Our results show that radiological densities of CD 117$^+$–enriched RAD 16I/collagen I samples were comparable to CT densities measured in healed fractured bones of the human hand after 6 weeks.[51] Others report an increase of radiological density in healed fractured bone after 1- and 2-year follow-up.[52] As our study was limited to 6 weeks but a steady increase in radiological density was observed, we speculate that further increase beyond 6 weeks would have been likely. We could not compare native bone from a human hand to our samples for biomechanical stiffness as no such human hand bone was available; however, stiffness was highest in CD 117$^+$–enriched RAD 16I/collagen I samples. Although only two samples of each hydrogel were tested biomechanically, the quality of new bone was confirmed by histologic results and radiologic findings. CD 117$^+$–enriched hMSCs were able to proliferate after being mixed directly into hydrogel and applied onto a scaffold. Thus, the time-consuming step of cell cultivation in flasks could possibly be avoided, and cells could be applied directly in the operating room onto preformed scaffolds.

Hydrogels provide a 3D structure for embedded cells and are used when tissue engineering bone.[16,23,24] Newly formed bone-like tissue mostly resembling native cortical bone was in the CD 117$^+$–enriched collagen I/RAD 16I specimens. This might be due to that RAD16I hydrogel has demonstrated in a variety of cells encapsulated and grown functional differentiation, such as bone, leading to extensive production of their own ECM.[18,19] Collagen I hydrogel has been described in literature as supporting bone formation.[53] As self-assembling peptide hydrogel, resulting nanofibers surround cells in a manner similar to ECM, which might, in combination with collagen I hydrogel, resemble native bone. Lesser new bone-like tissue was found in the CD 117$^+$–enriched collagen I and the CD 117$^-$ specimens. Collagen I is an essential component of native bone, and its abundance in hydrogels surrounding differentiated hMSCs proved to be beneficial for bone formation. The addition of RAD 16I seemed to support cellular proliferation in the hydrogel mix. Although RAD 16I pure hydrogel has qualities of similar ECM and support of cellular proliferation for various cell types,[18,19] pure RAD 16I did not support bone formation and had a low viscosity. Cells were forming clusters within the hydrogel. Using a mixture of collagen I/RAD 16I hydrogel, we achieved higher viscosity without compromising cellular proliferation. Cells did not proliferate in the same manner within collagen I. Bone-like tissue was formed mostly in the collagen I/RAD 16I mix. The results are confirmed by the biomechanical stiffness values in concordance with the VCT findings. The bone support may be due to collagen I hydrogel, as collagen is an essential part of bone.[6,10] Another reason might be the combination of RAD 16I with collagen I surrounding cells in a manner similar to ECM close to that of native bone.[18,19]

A limiting step in tissue engineering and regenerative medicine is cellular expansion in the laboratory.

In conclusion, we have demonstrated for the first time that it is possible to avoid the cell culture step and engineer bone *in vivo*. The combination of differentiated hBMSCs, enriched with CD 117$^+$ cells and placed in collagen I/RAD 16I hydrogel with 3DP β-TCP/PLGA scaffolds, can be used to engineer tissue that meets individual needs for bone reconstruction.

Acknowledgments

This study was funded by a Departmental Grant from the Department of Surgery, Massachusetts General Hospital. We would like to thank Dr. Frederic S. Shapiro, Children's Hospital, Boston, for the histopathological evaluation.

Disclosure Statement

Dr. Gupta served as consultant for Siemens Corporation, Forchheim, Germany. All authors have no conflicts of interest.

References

1. Montjovent, M.O., Burri, N., Mark, S., Federici, E., Scaletta, C., Zambelli, P.Y., Hohlfeld, P., Leyvraz, P.F., Applegate, L.L., and Pioletti, D.P. Fetal bone cells for tissue engineering. Bone **35,** 1323, 2004.
2. Aslan, H., Zilberman, Y., Kandel, L., Liebergall, M., Oskouian, R.J., Gazit, D., and Gazit, Z. Osteogenic differentiation of noncultured immunoisolated bone marrow-derived CD105$^+$ cells. Stem Cells **24,** 1728, 2006.
3. Pittenger, M.F., Mackay, A.M., Beck, S.C., Jaiswal, R.K., Douglas, R., Mosca, J.D., Moorman, M.A., Simonetti, D.W., Craig, S., and Marshak, D.R. Multilineage potential of adult human mesenchymal stem cells. Science **284,** 143, 1999.
4. Potten, C.S., and Morris, R.J. Epithelial stem cells *in vivo*. J Cell Sci **Suppl 10,** 45, 1988.

5. National Institutes of Health. Stem cell information—Appendix E: stem cell markers. Available at: http://stemcells.nih.gov/info/scireport/appendixE.asp. Accessed November 12, 2004.
6. Beresford, W.A. Bone formation. In: Histology. Available at: http://wberesford.hsc.wvu.edu/histolch8.htm. Accessed January 10, 2005.
7. Shizuru, J.A., Negrin, R.S., and Weissman, I.L. Hematopoietic stem and progenitor cells: clinical and preclinical regeneration of the hematolymphoid system. Annu Rev Med **56,** 509, 2005.
8. Huss, R., and Moosmann, S. The co-expression of CD117 (c-kit) and osteocalcin in activated bone marrow stem cells in different diseases. Br J Haematol **118,** 305, 2002.
9. Vlasselaer, P., Falla, N., Snoeck, H., and Mathieu, E. Characterization and purification of osteogenic cells from murine bone marrow by two-color cell sorting using anti-Sca-1 monoclonal antibody and wheat germ agglutinin. Blood **84,** 753, 1994.
10. Zghoul, N., van Griensven, M., Zeichen, J., Dittmar, K.E.J., Rohde, M., and Jaeger, V. 2005 Improved *in vitro* osteogenesis of multipotential human mesenchymal stem cells in three dimensional perfusion culture. Paper presented at the 2nd World Congress on Regenerative Medicine; May Leipzig, Germany. 2nd World Congress on Regenerative Medicine Paper no 130.
11. Watt, F.M., and Hogan, B.L.M. Out of Eden: stem cells and their niches. Science **287,** 1427, 2000.
12. Spradling, A., Drummond-Barbosa, D., and Kai, T. Stem cells find their niches. Nature **414,** 98, 2001.
13. Blackshaw, S.E., Arkinson, C., and Davis, C.J.A. Promotion of regeneration and axon growth following injury in an invertebrate nervous by the use of three-dimensional collagen gels. Proc R Soc Lond **264,** 657, 1997.
14. Dillon, G.P., Yu, W.M., Sridhan, J.P., Ranieri, R.V., and Bellamkonda, R.B. The influence of physical structure and charge on neurite extension in a 3D hydrogel. J Biomater Sci **9,** 1049, 1998.
15. Yu, X., Dillon, G.P., and Bellamkonda, R.B. A laminin and nerve growth factor-ladden three-dimensional scaffold for enhance neurite extension. Tissue Eng **5,** 291, 1999.
16. Botchwey, E.A., Dupree, M.A., Pollak, S.R., Levine, E.M., and Laurencin, C.T. Tissue engineered bone: measurement of nutrient transport in three dimensional matrices. J Biomed Mater Res **67A,** 357, 2003.
17. Zhang, S., Holmes, T.C., Lockshin, C., and Rich, A. Spontaneous assembly of a self-complementary oligopeptide to form a stable macroscopic membrane. Proc Natl Acad Sci **90,** 3334, 1993.
18. Zhang, S. Fabrication of novel biomaterials through molecular self-assembly. Nat Biotechnol **21,** 1171, 2003.
19. Holmes, T.C., Lacalle, S.D., Su, X., Liu, G., Rich, A., and Zhang, S. Extensive neurite outgrowth and active synapse formation on self-assembling peptide scaffolds. Proc Natl Acad Sci **99,** 9996, 2002.
20. Meinel, L., Karageorgiou, V., Fajardo, R., Snyder, B., Shinde-Patil, V., Zichner, L., Kaplan, D., Langer, R., and Vunjak-Novakovic, G. Bone tissue engineering using human mesenchymal stem cells: effects of scaffold material and medium flow. Ann Biomed Eng **32,** 112, 2004.
21. Terai, H., Hannouche, D., Ochoa, E., Yamano, Y., and Vacanti, J.P. *In vitro* engineering of bone using a rotational oxygen-permeable bioreactor system. Mater Sci Eng **C20,** 3, 2002.
22. Kreke, M.R., and Goldstein, A.S. Hydrodynamic shear stimulates osteocalcin expression but not proliferation of bone marrow stromal cells. Tissue Eng **10,** 780, 2004.
23. Weinand, C., Pomerantseva, I., Neville, C.M., Gupta, R., Weinberg, E., Madisch, I., Abukawa, H., Troulis, M.J., and Vacanti, J.P. Hydrogel–β-TCP scaffolds and stem cells for tissue engineering bone. Bone **38,** 555, 2006.
24. Weinand, C., Gupta, R., Huang, A., Weinberg, E., Qudsi, R., Neville, C.M., Pomerantseva, I., and Vacanti, J.P. Comparison of hydrogels in the *in vivo* formation of tissue engineered bone using mesenchymal stem cells and β-TCP scaffolds. Tissue Eng **13,** 757, 2007.
25. Lorenz, H.P., Hedrick, M.H., Chang, J., Mehrara, B.J., and Longaker, M.T. The impact of biomolecular medicine and tissue engineering on plastic surgery in the 21st century. Plast Reconstr Surg **105,** 2467, 2000.
26. Cima, L.G., Vacanti, J.P., Vacanti, C., Ingber, D., Mooney, D., and Langer, R. Tissue engineering by cell transplantation using degradable polymer substrates. J Biomech Eng **113,** 143, 1991.
27. Kim, W.S., Vacanti, J.P., Cima, L.G., Mooney, D., Upton, J., Puelacher, W.C., and Vacanti, C.A. Cartilage engineered in predetermined shapes employing cell transplantation on synthetic biodegradable polymers. Plast Reconstr Surg **94,** 233, 1994.
28. Shinoka, T., Ma, P.X., Shum-Tim, D., Breuer, C.K., Cusick, R.A., Zund, G., Langer, R., Vacanti, J.P., and Mayer, J.E. Tissue engineered heart valves. Autologous valve leaflet replacement study in a lamb model. Circulation **94,** 164, 1996.
29. Vacanti, C.A., and Upton, J. Tissue-engineered morphogenesis of cartilage and bone by means of cell transplantation using synthetic biodegradable polymer matrices. Clin Plast Surg **21,** 445, 1994.
30. Sherwood, J.K., Riley, S.L., Palazzolo, R., Brown, S.C., Monkhouse, D.C., Coates, M., Griffith, L.G., Landeen, L.K., and Ratcliffe, A. A three-dimensional osteochondral composite scaffold for articular cartilage repair. Biomaterials **23,** 4739, 2002.
31. Daigle, J.P., and Kleinert, J.M. Major limb replantation in children. Microsurgery **12,** 221, 1991.
32. Urbaniak, J.R. Replantation in children. In: Seraphin, D., and Georgiad, N.G., eds. Pediatric Plastic Surgery, vol. 2, St. Louis, MO: CV Mosby, pp. 1168–1186, 1984.
33. Schlenker, J.D., Kleinert, H.E., and Tsai, T.M. Methods and results of replantation following traumatic amputation of the thumb in sixty-four patients. J Hand Surg **5,** 63, 1980.
34. Benisse, L. Amputation. In: Lester, B., ed. The Acute Hand. Stamford, CT: Appleton & Lange, pp. 287–326, 1999.
35. Hentz, V.R. Replantation of digits. In: Hentz, V.R., and Chase, R.A., eds. Hand Surgery. A Clinical Atlas. Philadelphia, PA: W.B. Saunders Company, pp. 754–769, 2000.
36. Foucher, G., Merle, M., Maneaud, M., and Michon, J. Microsurgical free partial toe transfer in hand reconstruction: a report of 12 cases. Plast Reconstr Surg **65,** 616, 1980.
37. Hurwitz, P.J. Experimental transplantation of small joints by microvascular anastomoses. Plast Reconstr Surg **64A,** 221, 1979.
38. Mathes, S.J., Buchanan, R., and Weeks, P.M. Microvascular joint transplantation with epiphyseal growth. J Hand Surg **5,** 586, 1980.
39. O'Brien, B.M. Microvascular free small joint transfer. In: O'Brien, B.M., ed. Microvascular Reconstructive Surgery. New York: Churchill Livingston, 1977, pp. 284–289.

40. Vacanti, C.A., Bonassar, L.J., Vacanti, M.P., and Shufflebarger, J. Replacement of an avulsed phalanx with tissue-engineered bone. N Engl J Med **344,** 1511, 2001.
41. Perutelli, P., and Catellani, S. Leukocyte recovery from umbilical cord blood by poligeline. Hematol Cell Ther **41,** 1, 1999.
42. Li, T.S., Hayashi, M., Liu, Z.L., Ito, H., Mikamo, A., Furutani, A., Matsuzaki, M., and Hamano, K. Low angiogenic potency induced by the implantation of *ex-vivo* expanded CD 117^{+} stem cells. Am J Physiol Heart Circ Physiol **286,** 1236, 2004.
43. Rosen, K.M., and Villa-Komaroff, L. An alternative method for the visualization of RNA in formaldehyde agarose gels. Focus **845,** 23, 1990.
44. Klein, C.P., Driessen, A.A., de Groot, K., and van den Hooff, A. Biodegradation behavior of various calcium phosphate materials in bone tissue. J Biomed Mater Res **17,** 769, 1983.
45. Astete, C.E., and Sabliov, C.M. Synthesis and characterization of PLGA nanoparticles. J Biomater Sci Polym Ed **17,** 247, 2006.
46. Porter, B.D., Oldham, J.B., He, S.L., Zobitz, M.E., Payne, R.G., An, K.N., Currier, B.L., Mikos, A.G., and Yaszemski, M.J. Mechanical properties of a biodegradable bone regeneration scaffold. J Biomech Eng **122,** 286, 2000.
47. Dean, D., Topham, N.S., Meneghetti, S.C., Wolfe, M.S., Jepsen, K., He, S., Chen, J.E., Fisher, J.P., Cooke, M., Rimnac, C., and Mikos, A.G. Poly(propylene fumarate) and poly(DL-lactic-co-glycolic acid) as scaffold materials for solid and foam-coated composite tissue-engineered constructs for cranial reconstruction. Tissue Eng **9,** 495, 2003.
48. Lee, H.-S., Huang, G.-T., Chiang, H., Chiou, L.-L.,Chen, M.-H., Hsieh, C.-H., and Jiang, C.-C. Multipotential mesenchymal stem cells from femoral bone marrow near the site of osteonecrosis. Stem Cells **21,** 190, 2003.
49. Muschler, G.F., Matsukura, Y., Nitto, H., Boehm, C.A., Valdevit, A.D., Kambic, H.E., Davros, W.J., Easley, K.A., and Powell, K.A. Selective retention of bone marrow-derived cells to enhance spinal fusion. Clin Orthop Relat Res **432,** 242, 2005.
50. Rubio, D., Garcia-Castro, J., Martín, M.C., de la Fuente, R., Cigudosa, J.C., Lloyd, A.C., and Bernad, A. Spontaneous human adult stem cell transformation. Cancer Res **65,** 3035, 2005.
51. Madeley, N.J., Stephen, A.B., Downing, N.D., and Davis, T.R.C. Changes in scaphoid bone density after acute fracture. J Hand Surg [Br] **31,** 368, 2006.
52. Dirschl, D.R., Piedrahita, L., and Henderson, R.C. Bone mineral density 6 years after a hip fracture: a prospective, longitudinal study. Bone **26,** 95, 2000.
53. Hao, W., Hu, Y.-Y., We, Y.-Y., Pang, L., Lv, R., Bai, J.-P., Xiong, Z., and Jiang, M. Collagen I gel can facilitate homogenous bone formation of adipose-derived stem cells in PLGA-β-TCP scaffold. Cells Tissues Organs **187,** 89, 2008.

Address correspondence to:
Joseph P. Vacanti, M.D.
Laboratory for Tissue Engineering and Organ Fabrication
Harvard Medical School
Massachusetts General Hospital
55 Fruit St.
Boston, MA 02114

E-mail: jvacanti@partners.org

Received: August 13, 2008
Accepted: February 6, 2009
Online Publication Date: March 26, 2009